Exergy analysis of synthetic biofuel production via fast pyrolysis and hydroupgrading

CrossMark

Jens F. Peters [a], Fontina Petrakopoulou [b], Javier Dufour [a, c, *]

[a] Systems Analysis Unit, Instituto IMDEA Energía, Móstoles 28935, Spain
[b] Unit of Environmental Science and Technology, National Technical University of Athens, Athens 15773, Greece
[c] Department of Chemical and Energy Technology, Rey Juan Carlos University, Móstoles 28933, Spain

ARTICLE INFO

ABSTRACT

This paper presents the first assessment of the exergetic performance of a biorefinery process based on catalytic hydroupgrading of bio-oil from fast pyrolysis. Lignocellulosic biomass is converted into bio-oil through fast pyrolysis, which is then upgraded to synthetic fuels in a catalytic hydrotreating process. The biorefinery process is simulated numerically using commercial software and analyzed using exergetic analysis. Exergy balances are defined for each component of the plant and the exergetic efficiencies and exergy destruction rates are calculated at the component, section and plant level, identifying thermodynamic inefficiencies and revealing the potential for further improvement of the process. The overall biofuel process results in an exergetic efficiency of 60.1%, while the exergetic efficiency of the upgrading process in the biorefinery alone is 77.7%. Within the biorefinery, the steam reforming reactor is the main source of inefficiencies, followed by the two hydrotreating reactors. In spite of the high operating pressures in the hydrotreating section, the compressors have little impact on the total exergy destruction. Compared to competing lignocellulosic biofuel processes, like gasification with Fischer—Tropsch synthesis or lignocellulosic ethanol processes, the examined system achieves a significantly higher exergetic efficiency.

© 2014 Elsevier Ltd. All rights reserved.

1. Introduction

Biofuels are considered one of the key solutions for introducing renewable energies in the transport sector and thereby reducing its high dependency on fossil fuels. In order to achieve the target of 10% share of biofuels by 2020 set by the EU [1], the successful deployment of second generation biofuels is considered crucial [1—3]. Although still in the development phase, second generation biofuels offer high theoretical conversion efficiencies and allow the use of lignocellulosic feedstocks from waste and low input perennial energy crops [3,4]. A promising pathway for producing second generation biofuels is liquefaction of biomass via fast pyrolysis and the subsequent upgrading of the obtained bio-oil to high-quality blend-in fuel through hydrotreating [5—7]. This pathway results in high efficiency and good environmental performance [8—10]. Nevertheless, due to the difficult properties of the bio-oil, as for

example its thermal instability and tendency to coking and corresponding catalyst fouling, this process is still in the development phase [11,12]. Since, for this reason, no real operational data from existing plants are available, numerical simulation is necessary to assess such a process in detail.

Biomass is a limited resource, and it must thus be used in the most efficient way possible. An assessment of the operational efficiency of a biomass conversion process is of interest both for improving its performance and for comparing it with competing conversion processes. Exergetic analysis is a valuable tool for this purpose, as it detects thermodynamic irreversibilities in energy conversion systems and can be used to maximize operational efficiency. Although exergetic analysis has been widely applied to power plants and similar processes (e.g. Refs. [13,14]), it has had limited applications to conventional or even second generation biofuel processes [15—21]. This paper presents the simulation of a biorefinery process based on catalytic hydroupgrading of bio-oil from fast pyrolysis and the exergetic analysis and evaluation of the process. To the best of the authors' knowledge, this work represents the first assessment of the exergetic performance of this type of biorefinery process.

* Corresponding author. Systems Analysis Unit, Instituto IMDEA Energía, Móstoles 28935, Spain. Tel.: +34 91 7371117.
E-mail address: javier.dufour@imdea.org (J. Dufour).

2. Fast pyrolysis plant

The fast pyrolysis process that produces raw bio-oil has been assessed in a previous work [22]. The results of the pyrolysis process are included in this work in order to calculate efficiencies along the whole process chain (from biomass to synthetic fuel). In addition, information about pyrolysis yields and product composition is also presented.

In the **pyrolysis plant**, the biomass feedstock (hybrid poplar wood with 50% water content) is dried and ground before being converted into char, gas and bio-oil in a fast pyrolysis reactor. A schematic flowsheet of the pyrolysis plant is shown in Fig. 1. The pyrolysis reactor is a fluidized circulating bed reactor with recirculated pyrolysis gases used as fluidizing agent. The products are separated via a series of hot cyclones, a quench with recirculated bio-oil and a water cooler. The process heat for the pyrolysis reactor and the biomass dryer is provided by a combustor that burns the gas fraction plus part of the char product. Under fast pyrolysis conditions and a reactor temperature of 520 °C, 68.9% bio-oil, 13.4% gas, and 17.7% char (w/w) are obtained. Of the latter, 61% are burned together with the gas fraction, giving a net plant char yield of 6.6%. The obtained bio-oil has a carbon content of 52% (dry base), a water content of 19%, and a higher heating value of 17.7 MJ kg^{-1} [22].

3. Biorefinery plant

The biorefinery plant assessed in this paper upgrades raw bio-oil to fuel-grade synthetic gasoline and diesel. This is achieved by a two-stage catalytic hydrotreatment followed by the distillation of the hydrocarbon product to gasoline and diesel. A catalytic hydrocracker processes the heavy residue from the distillation. The hydrogen required for the hydrotreating and the hydrocracking reactor is produced through the steam reforming of the gas fractions and natural gas. The biorefinery process, simulated in Aspen Plus [23], is divided into three parts: the hydrotreating (HT) section, the hydrocracking and distillation (HC) section and the steam reforming (SR) section. Although in reality these three are sub-sections of the upgrading process in the biorefinery, for the purpose of the analysis here, they are regarded as separate processes. A schematic block diagram of the biorefinery process is presented in Fig. 2. The fast pyrolysis plant for the production of the bio-oil can be physically separated from the biorefinery, but it is also included in the assessment for calculating the overall process efficiency. The thermodynamic model chosen for the process simulation is RKS-BM, the most suitable model for the polar hydrocarbon mixtures processed in this biorefinery. Table 1 lists the main input data of the

simulation, while operational temperatures and pressures of the plant components can be derived from the stream tables of the Appendix (Tables A1–A3).

3.1. Hydrotreating (HT) section

In the HT section, the crude bio-oil is converted into almost oxygen-free hydrocarbon in a two-stage catalytic upgrading process. The Aspen Plus flowsheet of the HT section is shown in Fig. 3. The bio-oil (Stream HTBOILIN) is pressurized (HT-PUMP1) and preheated (HXC-HT3). It is then mixed with high-pressure hydrogen (Stream HPHYDROG) and further preheated (HXC-HT1) before entering the first stage hydrotreating reactor (HTREACT1). The reactor, operating under mild hydrotreating conditions (270 °C, 170 bar, commercial Co–Mo catalyst), stabilizes the bio-oil before its further processing in the second stage [6,24]. The stabilized oil, still with an oxygen content of 30%, is depressurized to 140 bar (HT-VALVE) and then deeply deoxygenized to less than 2% oxygen content in the second-stage hydrotreater (HTREACT2), operating at 350 °C and 140 bar (Co–Mo catalyst) [6,24]. A series of heat exchangers (HXC-HT1–HXC-HT3) and a water cooler (HXC-HT4) cool the product stream down condensing the contained water before a high-pressure flash unit (HT-FLASH) separates the aqueous and organic fractions. The necessary cooling of the highly exothermic hydrotreating reactors is provided by two steam circuits. One circuit generates high-pressure steam for heating the reboiler of the distillation column in the HC section (Stream HPSTEAM), while in the other one medium-pressure steam (Stream MPSTEAM1) is generated for external use (it cannot be used within the plant, since there is no demand for heat at this temperature in the biorefinery).

3.2. Hydrocracking and distillation (HC) section

In the HC section, the organic fraction from the HT section is refined into synthetic gasoline and diesel products. This is done via a two-stage distillation process. A catalytic hydrocracker further breaks up the heavy residue fraction from the distillation into lighter fractions, increasing thereby the final fuel yield. Fig. 4 shows the corresponding flowsheet of this section. The organic stream from the HT section (Stream HTORGANC) is separated into gas and liquid fractions in a flash unit (HC-FLASH). The liquid fraction is depressurized (HC-VALV1) and preheated (HXC-HC1 and HXC-HC2) before entering the first distillation column (HC-DIST1). In the distillation column, operating with 8 stages at atmospheric pressure, a gasoline product (Stream GASLNOUT) and a small fraction of incondensable gases (Stream DISTGAS) are obtained. The heavy
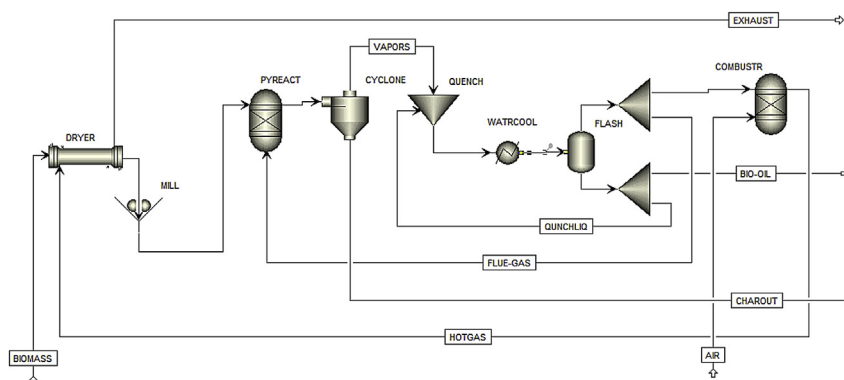
Fig. 1. Schematic flowsheet of the fast pyrolysis (PY) plant.
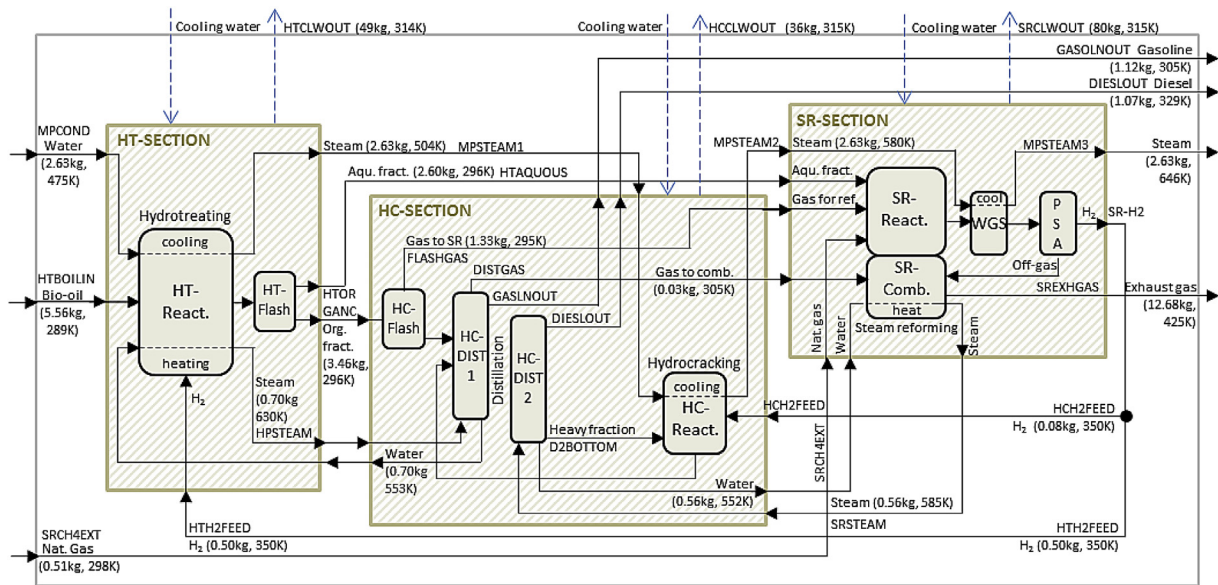
Fig. 2. Block diagram of the biorefinery process.

fraction passes through a valve (HC-VALV2) and is led to the second distillation column (HC-DIST2), operating with 9 stages at vacuum conditions. There, the diesel product (Stream DIESLOUT) and a heavy fraction (Stream D2BOTTOM) are obtained. Both columns are cooled by a water-cooling system, while heat for the reboilers is provided by high-pressure steam generated in the HT and the SR sections (Stream HPSTEAM/Q.HT-RCT and Stream SRSTEAM/Q-HXCSR4, respectively). The heavy fraction is pressurized (HC-PUMP3), mixed with high-pressure hydrogen and preheated (HXC-HC3). The mixture is then converted into small chain hydrocarbons in the hydrocracking reactor, operating at 400 °C and 90 bar with a commercial zeolite catalyst [25,26]. The product stream from the hydrocracker is depressurized (HC-VALV3), cooled (HXC-HC1, HXC-HC3) and recirculated (Stream CRACKOUT) to be mixed with the organic fraction exiting the HT section (HC-FLASH).

3.3. Steam reforming (SR) section

In the SR section, the hydrogen required by the HT and HC reactors is produced by reforming the process gases together with a small part of externally provided natural gas (methane). Fig. 5 shows the Aspen Plus flowsheet of the SR section. The gas fraction from the flash in the HC section (FLSHGAS) is split into a

fraction to be reformed (Stream SRGASRCT) and a fraction to be directly combusted (Stream SRGASCMB).

The fraction to be reformed is compressed (SR-COMP1) and mixed with steam (Stream SRVAPIN) and natural gas (Stream SRCH4EXT). The steam is produced from the aqueous fraction from the HT section (HTAQUOUS) and recycled excess water from the SR process (Stream SRH2OREC). After the mixer, the feed stream for the steam reformer is heated (HXC-SR2) and sent to the reactor (SR-REACT). In the reforming reactor, operating at 950 °C and 90 bar and using a Ni catalyst [27,28], the gases are converted into mainly CO and H_2. The high reforming temperature is required due to the high share of CO, CO_2 and the heavy hydrocarbon compounds in the stream. To increase the hydrogen yield further, the product stream is sent to a water-gas-shift reactor (SR-WGS), where the CO reacts with water to generate H_2 and CO_2. The product stream is cooled (HXC-SR1 and HXC-SR2) and the unreacted process water is condensed to separate it from the gas product (SR-COND). The gas stream is sent to the PSA (pressure swing adsorption) unit, where it is split into a hydrogen stream (Stream SR-H2), which is distributed between the HT and HC reactors (Streams HTH2FEED and HCH2FEED), and an off-gas stream (SROFFGS1). The off-gas stream is mixed (SR-MIX3) with combustion air (Stream SRCMBAIR), the gas stream from the first distillation column (Stream DISTGAS) and the gas fraction from the flash gases for direct combustion (Stream SRGASCMB). After it is preheated (HXC-SR3), this gas mixture enters the combustor where it is burned for generating the process heat required by the endothermic steam reforming reaction. In reality the combustion chamber is part of the steam-reforming reactor, but for simulation purposes, the two are modeled separately, connected with a heat stream. High-pressure steam (Stream SRSTEAM) is further generated (HXC-SR4) for producing the heat required by the distillation column reboiler (Q-HXCSR4).

4. Exergy calculations

Conventional energy analysis is based on the first law of thermodynamics. In contrast to energy, the concept of exergy is based on the second law of thermodynamics and considers the quality of energy in terms of obtainable work when a system is brought to thermodynamic equilibrium with its surroundings. In this way, an

Table 1
Main in- and output data of the simulation.

Parameter	Value/range
Air composition	0.21% O_2, 0.79% N_2
Ambient conditions	1 atm (1.01325 bar), 25 °C
Outlet temp cooling water	40 °C
Heat exchanger temp. approach	20 °C
Natural gas feed	100% CH_4, 50 bar
Electr. eff. pumps and compr.	98.5%
Isentropic compr. efficiency	72.0%
Pump efficiency	Aspen Plus estimation (eff. curve based on water)
Combustor thermal efficiency	85.0%
λ (excess oxygen for comb.)	20%
Gasoline yield	0.20 kg kg bio-oil^{-1}
Diesel yield	0.19 kg kg bio-oil^{-1}
Natural gas input	0.089 kg kg bio-oil^{-1}
Electricity input	0.64 kg kg bio-oil^{-1}

Fig. 3. Flowsheet of the hydrotreating (HT) section.

exergetic analysis permits the identification of the useful part of energy and pinpoints thermodynamic inefficiencies that energy analysis cannot detect [29–31].

The exergy of a stream is determined by four components: its potential, kinetic, physical and chemical exergy. In the analyzed process the kinetic and potential exergies of the streams are neglected and the exergy of a working fluid is assumed to be fully determined by its physical exergy, $\bar{e}_{ph}$, and chemical exergy, $\bar{e}_{ch}$.

All liquid streams included in the simulated process are considered to be ideal solutions. This simplification is made since the determination of activity coefficients for some of the bio-oil compounds, especially the degraded lignins, is extremely difficult. In general, the exergy of a fuel stream is determined by its chemical exergy, while the excess free enthalpy can be considered relatively small. For hydrocarbon fuels, the contribution of the excess enthalpy to their total exergy is only around 0.1–0.2%

[32]. For bio-oil, a more complex mixture of polar and non-polar compounds, this value would be somewhat higher. Still, neglecting this relatively small contribution is a valid simplification, especially since active separation processes (e.g., distillation) are only applied to near-ideal mixtures (hydrocarbon mixtures).

The internal database and the parameter estimation system of Aspen Plus are not equipped with exergy calculations. The specific exergies $\bar{e}$ of the streams are, therefore, calculated externally. For determining the **physical exergy** of the streams, the enthalpy and entropy values provided by Aspen Plus are used. The $\bar{e}_{ph}$ is then calculated according to Eq. (1), with h and s the mole-specific enthalpy and entropy, respectively.

$$\bar{e}_{ph} = (h - h_0) - T_0(s - s_0) \tag{1}$$
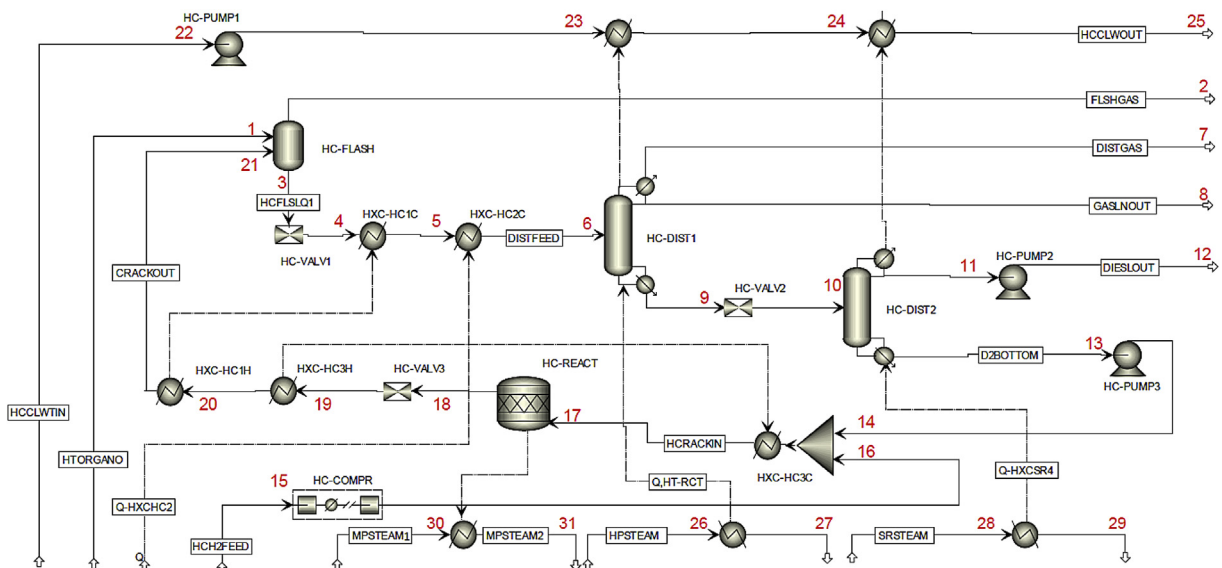
Fig. 4. Flowsheet of the hydrocracking and distillation (HC) section.
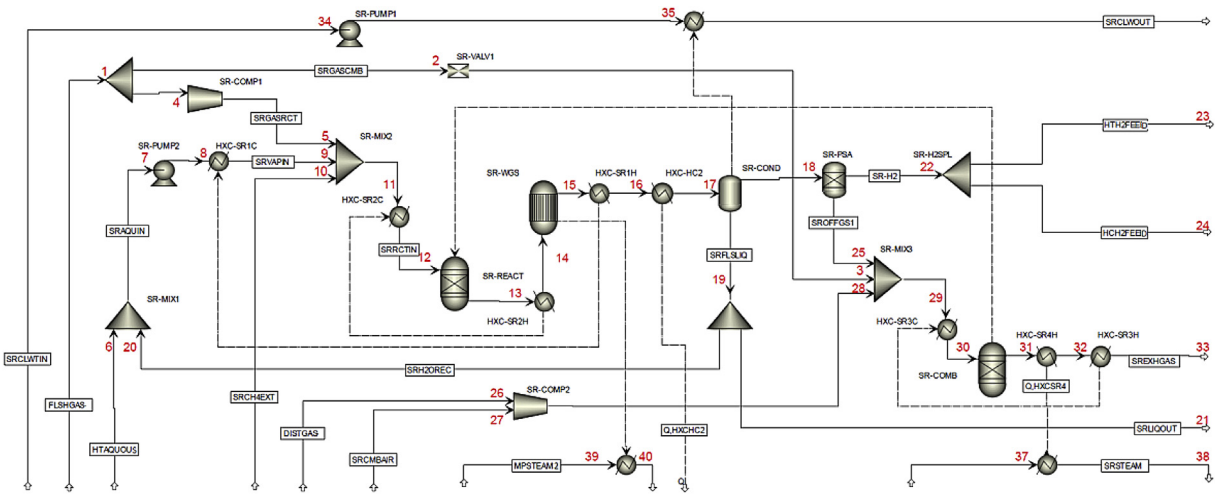
Fig. 5. Flowsheet of the steam reforming (SR) section.

The **chemical exergy** of the streams is calculated according to Eq. (2), with R the gas constant and x_i the mole fraction of compound i in the stream at T_0, p_0.

$$\bar{e}_{ch} = \sum x_i \bar{e}_{ch,i} + \bar{R} T_0 \sum x_i ln x_i \qquad (2)$$

Eq. (2) requires the determination of the chemical exergies of the compounds contained in a stream. For standard compounds $\bar{e}_{ch}$ is available in reference tables [33–35]. The model of Morris & Szargut [31] is used in this paper. The chemical exergy of compounds that are not listed in standard exergy tables is calculated based on the change in the Gibbs free energy ΔG or their atomic composition and higher heating value, depending on the property data that can be retrieved from the parameter estimation system of Aspen Plus. More details about the methodology and the chemical exergies calculated for some model compounds of the bio-oil can be found in Ref. [22].

The exergetic analysis is performed at the component level of the biorefinery plant. For the total process (tot) and for each individual plant component k, the rate of the **exergy of the fuel** ($\dot{E}_{F,tot}$, $\dot{E}_{F,k}$), and the rate of **exergy of the product** ($\dot{E}_{P,tot}$, $\dot{E}_{P,k}$) are determined. For standard components like, for example, heat exchangers or pumps, the balances are clearly determined and can be found in reference literature [29,30,36,37]. For components like distillation columns and reactors, the balances can differ based on their specific operation. The stream balances defined for each component of the process can be found in Table A4 of the Appendix. Based on the exergy of the fuel and product calculations, the rate of **exergy destruction** within each component k, ($\dot{E}_{D,k}$), and the whole process ($\dot{E}_{D,tot}$) is calculated as the difference between the rate of exergy of the fuel and the product. **Exergy loss** is the exergy of the streams that cross the system boundaries and is rejected to the environment. These streams are not part of the exergy of the product and they are not used within the system. Finally, the **exergetic efficiency** of component k (ε_k) and the overall process (ε_{tot}) is calculated as the ratio between the exergy of the product and the exergy of the fuel [30]. This definition is similar to the 'rational efficiency' of Kotas [34] and differs from the simple efficiency, where all outflows are considered part of the product.

To further assess the exergetic performance of a system, the **exergy destruction ratio** ($y_{D,k}$) and the **exergy loss ratio** (y_L) are calculated (the latter only for the overall biofuel system) as the rates of exergy destruction and exergy loss divided by the rates of

exergy of the fuel. The exergy destruction ratio reveals the contribution of each component to the reduction of the exergetic efficiency of the plant. It is, thereby, a useful tool for comparing different plant components indicating the relative importance of the components in the overall system. For the same purpose, the **relative exergy destruction ratio** ($y^*_{D,k}$) is calculated for each component as the rate of exergy destruction within the component over the overall exergy destruction rate within the system. More details about the principles of exergetic analysis, the definition of exergetic efficiencies and exergy balances for standard components of power plants can be found in literature [29,30,36,38–40].

5. Results and discussion

5.1. Fast pyrolysis process

The fast pyrolysis process results in an exergy destruction rate $\dot{E}_D$ of 43,054 kW. This, with a fuel exergy rate $\dot{E}_F$ of 157,708 kW, corresponds to an exergetic efficiency of 70.6%, and an exergy destruction ratio y_D of 22.9%. The exergy loss rate of the pyrolysis process $\dot{E}_{L,PYR}$, if considered as a separated system, is 3247 kW, resulting in an exergy loss ratio y_L of 1.7%. Detailed results for the pyrolysis process can be found in Ref. [22]. It is found that most of the exergy destruction (36.7% of the total exergy destroyed) takes place in the gas-and-char combustor. The irreversibilities within the pyrolysis reactor itself are responsible for 12% of the overall exergy destruction and are therefore less significant. Furthermore, 11% of the exergy destruction is caused by the dissipative cooling that is required in the bio-oil recovery section [41]. The components with the highest potential for improvement are the biomass dryer and the mill, responsible for 15.7% and 2.8% of the total exergy destruction in the pyrolysis plant, respectively. The high air flow required by the dryer is one of the reasons of the high exergy destruction within the air preheater of the combustion process (mainly due to the combined effect of pressure drops and high air flow). The remaining components (i.e., pumps and compressors) have rather small influence on the performance of the pyrolysis plant, with the exception of the combustion air compressor. Hence, reducing the heat demand of the dryer (by using dryer feedstock or by reducing the drying intensity) would reduce the inefficiencies of the pyrolysis plant significantly and would be the first step for improving its performance [22].

5.2. Biorefinery

The three sections of the biorefinery are assessed individually, revealing the efficiencies for each section and the contribution of individual components to the total exergy destruction within the section. Nevertheless, it must be noted that they form part of one single biorefinery plant and that heat exchange takes place among the three sections. The boundaries of the different sections and of the overall biorefinery process, together with their main in- and outflows are indicated in Fig. 2.

5.2.1. Hydrotreating (HT) section

For the HT section, an exergetic efficiency of 85.9% (Table 2) is calculated. The components that contribute most to the inefficiencies of this section are the two HT reactors, responsible for 64.9% and 21.6% of the exergy destruction of the section and the whole biorefinery, respectively. The main cause of exergy destruction is the chemical reactions, resulting in low exergetic efficiencies for the reactors (13.6% and 41.1%). The different efficiencies obtained for the two reactors can be partially attributed to the reactor cooling system, which uses a single cooling water stream for cooling both reactors. In consequence, the HTREACT1 acts as a pre-heater for the cooling water stream, while the second reactor, HTREACT2, fully evaporates the water, producing steam and therewith achieving a higher exergy increase in the water cooling circuit.

The heat exchangers show relatively high efficiencies, with the exception of the HXC-HT3. Low heat exchanger efficiencies indicate a poor heat integration of the process. Nevertheless, in the given case some inefficiencies concerning heat integration are assumed in order to achieve a more flexible process structure. Improvements could, hence, be achieved by a more rigorous heat integration that does not require operational flexibility. On the other hand, this would limit the operation of the plant to a given bio-oil feed composition and would require the re-adjustment of the operational parameters with every change in the bio-oil feed. Increasing the efficiency of the steam production (the cooling of the hydrotreating reactors) could result in further improvements, although this would apply to all heat generating processes. Further improvement is rather difficult to achieve, since the exergy destruction within the flash unit and the valves is mainly associated with pressure drops, while pumps and compressors are responsible for only 1% of the exergy destruction within this section (in spite of the high operational pressures required in the HT section).

5.2.2. Hydrocracking and distillation (HC) section

The HC section results in an efficiency of 85.4%. Since it is responsible for only 1.3% of the total destruction of the exergy of fuel in the biorefinery (Table 3), the potential for improving the

performance of the overall process through the improvement of this section is rather low. The main contributors to the total inefficiencies in this section are the two distillation columns, responsible together for more than 50% of the exergy destruction in this section.

The efficiencies of the heat exchangers in the feed stream of the distillation column are 51.3% and 60.8%. These heat exchangers are given low priority in the heat integration process due to their low enthalpy rates and their relatively low efficiency. To achieve a better match for the corresponding streams, additional heat exchangers would be required. However, this is not examined, as their contribution to the total destruction of the exergy of the fuel in the biorefinery is only 0.1%.

The hydrocracker involves chemical reactions associated with significant exergy destruction and achieves an exergetic efficiency of 50.3%. Nevertheless, the stream flow passing through the component is rather low. This component has, therefore, only a small contribution to the overall inefficiencies of the section and, consequently, the overall plant.

A significant contribution to the inefficiencies of the section is also found for the feed mixer and flash (HC-FLASH), mainly due to the high pressure drop within this component. Nevertheless, this pressure drop (and the associated exergy destruction) is unavoidable as the high pressure streams from the HT section must be depressurized for the distillation that takes place at ambient pressure.

Finally, the distillation columns show rather low exergetic efficiencies. However, distillation columns are generally exergetically inefficient, with efficiencies typically reaching 20–25% [42]. Compared with these values, the results obtained for the distillation columns are within the normal range. The potential for further improvement of the distillation columns is therefore limited. However, although the two distillation columns are responsible for almost half of the total exergy destruction within this section, they destroy only 0.7% of the exergy of the fuel of the overall biorefinery system. A more rigorous optimization of the columns is therefore not examined, as this would reduce the flexibility of the system.

5.2.3. Steam reforming (SR) section

60.4% of the total exergy destruction within the biorefinery is associated with the SR section (Table 4). Nevertheless, the exergetic efficiency of this section is relatively high (81.7%). The steam-reforming reactor, and especially the included combustion process that generates process heat, is the component with the highest contribution to the total exergy destruction within this section (43.6%). The WGS reactor, on the other hand, is responsible for the

Table 2
Exergy results of the hydrotreating (HT) section.[a]

Component	$\dot{E}_P$ (kW)	$\dot{E}_F$ (kW)	$\dot{E}_D$ (kW)	$y^*_{D,k}$ (%)	ε (%)	$y_{D,k}$ (%)
HT-PUMP1	103	200	97	0.4	51.7	0.1
HT-COMPR	1002	1648	646	2.4	60.8	0.5
HXC-HT1	1438	1823	384	1.4	78.9	0.3
HTREACT1	390	2870	2479	9.3	13.6	1.9
HT-VALVE	0	173	173	0.6	–	0.1
HXC-HT2	710	913	204	0.8	77.7	0.2
HTREACT2	2295	5586	3291	12.3	41.1	2.6
HXC-HT3	208	515	307	1.1	40.4	0.2
HXC-HT4	93	726	633	2.4	12.8	0.5
HT-FLASH	0	671	671	2.5	–	0.5
HT-PUMP2	5	6	1	0.0	77.2	0.0
HT section	**53,909**	**62,788**	**8887**	**33.2**	**85.9**	**6.9**

^a The exergy destruction ratios *y* and *y** are given in relation to the overall biorefinery system.

Table 3
Exergy results of the distillation and hydrocracking (HC) section.[a]

Component	$\dot{E}_P$ (kW)	$\dot{E}_F$ (kW)	$\dot{E}_D$ (kW)	$y^*_{D,k}$ (%)	ε (%)	$y_{D,k}$ (%)
HC-COMPR	103	131	27	0.1	79.1	0.0
HC-PUMP1	7	10	3	0.0	73.6	0.0
HC-FLASH	0	294	294	1.1	–	0.2
HC-VALV1	0	2	2	0.0	–	0.0
HXC-HC1	34	66	32	0.1	51.3	0.0
HXC-HC2	104	172	67	0.3	60.8	0.1
HC-DIST1	153	612	458	1.7	25.0	0.4
HC-VALV2	0	153	153	0.6	–	0.1
HC-DIST2	73	434	361	1.3	16.7	0.3
HC-PUMP2	0	1	0	0.0	40.5	0.0
HC-PUMP3	5	9	3	0.0	61.4	0.0
HC-REACT	190	379	188	0.7	50.3	0.1
HXC-HC3	316	385	69	0.3	82.0	0.1
HC-VALV3	0	71	71	0.3	–	0.1
HC section	**9084**	**10,643**	**1731**	**6.5**	**85.4**	**1.3**

^a The exergy destruction ratios *y* and *y** are presented in relation to the overall biorefinery system.

Table 4
Exergy results of the steam-reforming (SR) section.[a]

Component	$\dot{E}_P$ (kW)	$\dot{E}_F$ (kW)	$\dot{E}_D$ (kW)	$y_{D,k}^*$ (%)	ε (%)	$y_{D,k}$(%)
SR-MIX1	0	23	23	0.1	–	0.0
SR-PUMP2	10	18	8	0.0	54.1	0.0
SR-COMP1	525	676	152	0.6	77.6	0.1
SR-MIX2	0	593	593	2.2	–	0.5
HXC SR-2	5571	8597	3026	11.3	64.8	2.4
SR-VALV1	0	87	87	0.3	–	0.1
SR-REACT	12,719	19,768	7049	26.3	64.3	5.5
SR-WGS	192	586	394	1.5	32.7	0.3
HXC SR-1	1984	2492	508	1.9	79.6	0.4
SR-COMP2	882	1157	275	1.0	76.2	0.2
SR-COND	0	1456	1456	5.4	9.7	1.1
SR-PSA	0	441	441	1.6	–	0.3
HXC SR-4	415	1066	651	2.4	38.9	0.5
HXC SR-3	8200	8943	743	2.8	91.7	0.6
SR-MIX3	0	705	705	2.6	–	0.5
SR-PUMP1	7	9	2	0.0	80.0	0.0
SR-H2SPL	0	48	48	0.2	–	0.0
SR section	**72,732**	**89,068**	**16,161**	**60.4**	**81.7**	**12.6**

[a] The exergy destruction ratios y and y^* are presented in relation to the overall biorefinery system.

destruction of only 0.3% of the exergy of the fuel ($y_{D,SR\text{-}WGS}$) of the overall biorefinery system. Smaller, but still considerable exergy destruction is calculated for the feed mixers, where streams of different temperatures and compositions are mixed (see Table A.4 in the Appendix). A better adjustment of the inlet stream temperatures could reduce the inefficiencies in these components, but would require additional heat exchangers increasing the pressure drops and the financial expenditure of the section. Since the contribution of the mixers to the destruction of the exergy of the fuel of the whole biorefinery plant is only about 1%, it is not further assessed as an improvement measure.

High exergy destruction is also found in the heat exchanger that preheats the inlet stream of the SR-reactor (HXC SR-2). Its rather low efficiency of 64.8% is a result of a heat capacity mismatch between its feed and product streams due to their different water contents (the SR reaction consumes significant amounts of water). Nevertheless, a better match of heat streams is not possible in the simulated plant, as streams of other sections show very different compositions and/ or mass flows that would result in worse results. In this sense, the matching of the streams is a result of the water consuming reaction and can be improved only with additional heat exchangers and for a plant under constant conditions (no changes in the feedstock composition). The condenser, SR-COND, contributes the third largest share to the exergy destruction within this section. Since it is a dissipative component, whose purpose is the separation of the water contained in the product stream by condensing it, the definition of an exergetic efficiency for this component is not possible.

5.3. Overall biofuel system

Although the three sections of the biorefinery are assessed individually, heat exchange takes place among the three sections. The results of the exergetic analysis for the complete biofuel chain (fast pyrolysis and upgrading of the bio-oil to synthetic fuel) are shown in Table 5. The overall biofuel system achieves an exergetic efficiency of 60.1%, with the upgrading process in the biorefinery process showing a slightly higher efficiency than the pyrolysis plant. The exergy destruction ratio $y_{D,tot}$ indicates that 37.1% of the exergy of the fuel is destroyed in the overall process chain, while another 2.7% is rejected unused to the environment (exergy loss ratio; $y_{L,tot}$). When considering only the main products, the synthetic gasoline and diesel (i.e. omitting the char and steam by-products), the exergetic efficiency achieved is 51.8%.

Table 5
Results of the exergetic analysis for the overall biofuel system.

Section	$\dot{E}_P$ (kW)	$\dot{E}_F$ (kW)	$\dot{E}_D$ (kW)	y_D^*	$\dot{E}_L$ (kW)	ε (%)	y_D (%)	y_L (%)
Pyrolysis	111,407	157,708	43,054	61.7%	3247	70.6	22.9	1.7
Biorefinery	99,872	128,573	26,778	38.3%	1923	77.7	14.2	1.0
Overall process	**113,085**	**188,087**	**69,833**	**100.0%**	**5169**	**60.1**	**37.1**	**2.7**

The upgrading process in the biorefinery is responsible for only 38% of the overall exergy destruction. For the exergy losses, a similar pattern can be found, with 37% of the overall losses originating in the biorefinery and 63% in the pyrolysis plant. Within the biorefinery, the main source of inefficiencies is the SR section, responsible for more than 60% of the total exergy destruction within the biorefinery. Main source of these inefficiencies is the SR reactor. Nevertheless, an important part of the exergy (about one third) is also destroyed in the HT section, mainly due to the chemical reactions within the HT reactors. Inefficiencies in the HC section are rather low and contribute less than 7% to the total. Reducing the hydrogen demand of the HT reactions by, e.g., specially tailored catalysts would hence reduce the inefficiencies of both the HT and the SR reactors and improve the efficiency of the biorefinery system.

The exergetic efficiency obtained for the pyrolysis biofuel process chain is, with 60.1%, among the highest reported for lignocellulosic biofuel processes, comparable with the production of hydrogen or synthetic methane via gasification, which can reach values of up to 66% [43,44]. However, such technologies obtain gaseous fuels and are, therefore, less suitable for substituting fossil fuels in the transport sector. In comparison with alternative processes for obtaining liquid biofuels, the efficiency obtained for the biofuel process chain is significantly higher. For a typical FT-process, based on the gasification of biomass and subsequent FT-synthesis to synthetic biofuels, efficiencies between 28% and 46% are reported in literature [21,41,45–47]. The mentioned values depend on the layout of the process and the type of the feedstock. The catalytic synthesis of methanol from the gasification products can reach 56% [43,48]. For lignocellulosic ethanol processes, a wider range can be found in literature, depending on the use of the lignin residue obtained from the process. Considering the residue as energy by-product gives higher efficiencies than its combustion for heat and/or electricity generation. In any case, lignocellulosic ethanol processes achieve efficiencies between 12 and 44%, still somewhat lower than those of FT-processes [49–54].

6. Conclusion

The exergetic efficiency of the overall biofuel system including pyrolysis and upgrading is 60.1% for a feedstock with 50% water content. The pyrolysis shows the highest contribution to the overall inefficiencies, specifically related to the included combustor and dryer. Within the biorefinery, the steam reforming process has the highest contribution to the overall exergy destruction, mainly due to the steam-reforming reactor and the associated heat exchangers. In general, the processes that involve chemical reactions, above all the reactors where combustion takes place, result in high exergy destruction. Other reactors, like the hydrotreating and hydrocracking reactors, show even lower exergetic efficiencies, but their contribution to the overall inefficiencies is relatively low.

It is found that, to improve the performance of the biorefinery system, priority should be given to improvements within the steam reforming section. The reduction of the hydrogen demand and/or the hydrogen excess in the hydrotreating reactors could be measures with positive results in this regard. Such measures would require the

variation of the operational conditions of the reactors and would affect the yields and compositions of the hydrotreating products. An explicit assessment of this aspect would therefore be required for a well-founded recommendation on this aspect. However, it can be expected that reducing hydrogen requirements would reduce the inefficiencies in the steam reformer and the associated heat exchangers significantly. Furthermore, a more rigorous heat integration would improve the overall efficiency, but, most probably, at the expense of the operational flexibility and process structure.

On the other hand, the highest potential for improvement is identified for the pyrolysis plant, which is found to be responsible for most of the exergy destruction within the overall process chain. Furthermore, since the biomass pretreatment is one of the main sources of inefficiency in the pyrolysis plant, reducing the drying requirements by, e.g., using wood with lower moisture content, would be the most straightforward measure to increase the performance of the overall system.

In general, the production of synthetic biofuels via pyrolysis and hydroupgrading shows an exergetic efficiency significantly higher than those reported in literature for alternative lignocellulosic biofuel processes. At the same time, significant improvement potential is still present. The examined system can hence be considered a thermodynamically promising pathway for the production of lignocellulosic biofuels.

Acknowledgment

Nomenclature

Symbols

$\bar{e}$	specific exergy (kJ/kmol)
$\dot{E}$	exergy rate (kW)
ε	exergetic efficiency (%)
ΔG	change in Gibbs energy (kJ/kmol)
$\bar{h}$	specific enthalpy (kJ/kmol)
$\dot{m}$	mass flow rate (kg/s)
$\dot{n}$	mole flow rate (kmol/s)
p	pressure (bar)
R	gas constant (J/mol K)
$\bar{s}$	specific entropy (kJ/kmol K)
T	temperature (°C)
vf	vapor fraction
x	mole fraction
y	exergy destruction ratio (%)
y^*	relative exergy destruction (%)

Subscripts

c	char
ch	chemical (exergy)
D	destruction (exergy)
F	fuel (exergy)
i	compound
k	component
L	loss (exergy)
m	mass
n	amount of substance (moles)
P	product (exergy)
p	pressure
ph	physical (exergy)
w	wood
wt	weight basis
tot	total (overall process)
0	reference thermodynamic environment

Appendix

Stream tables used for the calculation of the exergy balances. Note that the stream numbering of each section starts with 1.

Table A1
Stream tables of the HT section.

		1	2	3	4	5	7	8	9	10	11
T	K	289.3	297.4	400.0	350.0	425.0	525.0	523.2	576.8	572.7	645.2
p	bar	1.061	171.000	171.000	44.500	170.500	169.500	168.600	167.900	140.000	139.100
$\dot{m}$	kg/s	5.56	5.56	5.56	0.50	0.50	6.06	6.06	6.06	6.06	6.06
$\dot{n}$	kmol/s	0.11	0.11	0.11	0.25	0.25	0.36	0.38	0.38	0.38	0.33
vf		0.00	0.00	0.00	1.00	1.00	0.88	0.88	0.97	0.97	1.00
e_{ph}	kJ/kmol	1.88E+01	9.60E+02	2.86E+03	9.57E+03	1.36E+04	1.44E+04	1.40E+04	1.57E+04	1.52E+04	1.69E+04
e_{ch}	kJ/kmol	8.95E+05	8.95E+05	8.95E+05	2.36E+05	2.36E+05	4.38E+05	4.08E+05	4.08E+05	4.08E+05	4.43E+05
$\dot{E}$	kJ/s	9.82E+04	9.83E+04	9.85E+04	6.09E+04	6.19E+04	1.62E+05	1.50E+05	1.60E+05	1.60E+05	1.54E+05
h	kJ/kmol	−3.61E+05	−3.59E+05	−3.45E+05	1.55E+03	3.93E+03	−9.06E+04	−8.81E+04	−8.30E+04	−8.30E+04	−1.14E+05
s	kJ/kmol K	−2.78E+02	−2.75E+02	−2.36E+02	−2.69E+01	−3.24E+01	−6.71E+01	−5.72E+01	−4.79E+01	−4.64E+01	−5.42E+01

		12	13	14	15	16	17	18	19	20	21
T	K	550.0	473.2	440.0	305.0	295.9	295.9	475.0	484.8	504.6	298.5
p	bar	138.800	138.100	138.100	137.400	35.000	35.000	20.000	20.000	20.000	1.013
$\dot{m}$	kg/s	6.06	6.06	6.06	6.06	3.46	2.60	2.63	2.63	2.63	49.27
$\dot{n}$	kmol/s	0.33	0.33	0.33	0.33	0.19	0.14	0.15	0.15	0.15	2.74
vf		0.98	0.69	0.63	0.57	1.00	0.00	0.00	0.11	1.00	0.00
e_{ph}	kJ/kmol	1.42E+04	1.05E+04	9.19E+03	6.95E+03	8.69E+03	8.28E+01	3.47E+03	4.30E+03	8.58E+03	0.00E+00
e_{ch}	kJ/kmol	4.43E+05	4.42E+05	4.41E+05	4.41E+05	7.61E+05	1.21E+04	9.00E+02	1.81E+03	9.50E+03	9.00E+02
$\dot{E}$	kJ/s	1.53E+05	1.51E+05	1.51E+05	1.50E+05	1.48E+05	1.75E+03	6.37E+02	8.91E+02	2.64E+03	2.46E+03
h	kJ/kmol	−1.20E+05	−1.33E+05	−1.37E+05	−1.49E+05	−4.71E+04	−2.85E+05	−2.73E+05	−2.68E+05	−2.36E+05	−2.89E+05
s	kJ/kmol K	−6.38E+01	−9.03E+01	−1.00E+02	−1.30E+02	−8.79E+01	−1.72E+02	−1.29E+02	−1.20E+02	−5.24E+01	−1.71E+02

		22	23	24	25
T	K	298.5	314.4	552.8	620.0
p	bar	1.713	1.063	70.000	70.000
$\dot{m}$	kg/s	49.27	49.27	0.70	0.70

Table A1 (*continued*)

		22	23	24	25
$\dot{n}$	kmol/s	2.74	2.74	0.04	0.04
vf		0.00	0.00	0.00	1.00
e_{ph}	kJ/kmol	1.69E+00	3.57E+01	7.02E+03	1.26E+04
e_{ch}	kJ/kmol	9.00E+02	9.00E+02	9.00E+02	9.50E+03
$\dot{E}$	kJ/s	2.47E+03	2.56E+03	3.08E+02	8.58E+02
h	kJ/kmol	−2.89E+05	−2.87E+05	−2.65E+05	−2.33E+05
s	kJ/kmol K	−1.71E+02	−1.66E+02	−1.14E+02	−5.71E+01

Table A2
Stream tables of the HC section.

		1	2	3	4	5	6	7	8	9	10
T	K	295.9	295.2	295.2	296.0	364.0	430.0	305.0	305.0	532.0	450.8
p	bar	35.000	20.000	20.000	6.000	4.600	3.900	2.300	2.300	2.825	0.030
$\dot{m}$	kg/s	3.46	1.33	2.40	2.40	2.40	2.40	0.03	1.12	1.26	1.26
$\dot{n}$	kmol/s	0.19	0.20	0.02	0.02	0.02	0.02	0.00	0.01	0.01	0.01
vf		0.89	1.00	0.00	0.04	0.28	1.00	0.00	0.00	0.00	0.79
e_{ph}	kJ/kmol	7.95E+03	7.42E+03	3.37E+02	1.38E+02	1.68E+03	6.52E+03	2.02E+03	2.82E+01	2.65E+04	3.57E+03
e_{ch}	kJ/kmol	7.62E+05	2.81E+05	5.16E+06	5.16E+06	5.16E+06	5.17E+06	6.97E+05	3.93E+06	7.90E+06	7.91E+06
$\dot{E}$	kJ/s	1.48E+05	5.85E+04	1.06E+05	1.06E+05	1.06E+05	1.06E+05	5.44E+02	4.98E+04	5.57E+04	5.55E+04
h	kJ/kmol	−5.11E+04	−3.28E+04	−1.70E+05	−1.70E+05	−1.54E+05	−1.30E+05	−2.08E+05	−1.46E+05	−1.10E+05	−1.10E+05
s	kJ/kmol K	−9.72E+01	−2.74E+01	−6.97E+02	−6.96E+02	−6.48E+02	−5.88E+02	−6.14E+01	−5.42E+02	−8.11E+02	−7.90E+02

		11	12	13	14	15	16	17	18	19	20
T	K	329.3	329.5	551.1	567.8	350.0	461.0	870.0	948.2	950.4	510.6
p	bar	0.010	1.216	0.020	90.000	44.500	90.000	89.750	88.850	36.000	35.696
$\dot{m}$	kg/s	1.07	1.07	0.19	0.19	0.08	0.08	0.27	0.27	0.27	0.27
$\dot{n}$	kmol/s	0.01	0.01	0.00	0.00	0.04	0.04	0.04	0.03	0.03	0.03
vf		0.00	0.00	0.00	0.00	1.00	1.00	1.00	1.00	1.00	1.00
e_{ph}	kJ/kmol	4.77E+02	5.16E+02	3.04E+04	3.68E+04	9.57E+03	1.22E+04	2.10E+04	2.57E+04	2.35E+04	1.10E+04
e_{ch}	kJ/kmol	7.73E+06	7.73E+06	9.15E+06	9.15E+06	2.36E+05	2.36E+05	4.26E+05	5.34E+05	5.34E+05	5.34E+05
$\dot{E}$	kJ/s	4.77E+04	4.77E+04	7.78E+03	7.78E+03	9.53E+03	9.63E+03	1.77E+04	1.74E+04	1.73E+04	1.69E+04
h	kJ/kmol	−2.47E+05	−2.47E+05	2.70E+05	2.80E+05	1.55E+03	4.87E+03	2.74E+04	2.14E+04	2.14E+04	6.36E+01
s	kJ/kmol K	−1.07E+03	−1.07E+03	−3.69E+02	−3.56E+02	−2.69E+01	−2.47E+01	−6.46E+00	−2.16E+01	−1.40E+01	−4.37E+01

		21	22	23	24	25	26	27	28	29	30	31
T	K	305.0	298.5	298.5	306.4	314.9	620.0	552.8	585.0	551.5	503.9	579.3
p	bar	35.696	1.013	2.513	1.863	1.213	70.000	70.000	70.000	70.000	20.000	20.000
$\dot{m}$	kg/s	0.27	35.58	35.58	35.58	35.58	0.70	0.70	0.56	0.56	2.63	2.63
$\dot{n}$	kmol/s	0.03	1.98	1.98	1.98	1.98	0.04	0.04	0.03	0.03	0.15	0.15
vf		0.95	0.00	0.00	0.00	0.00	1.00	0.00	1.00	0.00	1.00	1.00
e_{ph}	kJ/kmol	8.50E+03	0.00E+00	3.58E+00	1.09E+01	3.83E+01	1.26E+04	7.02E+03	1.17E+04	6.95E+03	8.57E+03	9.87E+03
e_{ch}	kJ/kmol	5.34E+05	9.00E+02	9.00E+02	9.00E+02	9.00E+02	9.50E+03	9.00E+02	9.50E+03	9.00E+02	9.50E+03	9.50E+03
$\dot{E}$	kJ/s	1.68E+04	1.78E+03	1.78E+03	1.80E+03	1.85E+03	8.58E+02	3.08E+02	6.60E+02	2.44E+02	2.64E+03	2.83E+03
h	kJ/kmol	−1.06E+04	−2.89E+05	−2.89E+05	−2.88E+05	−2.87E+05	−2.33E+05	−2.65E+05	−2.35E+05	−2.65E+05	−2.36E+05	−2.33E+05
s	kJ/kmol K	−7.00E+01	−1.71E+02	−1.71E+02	−1.68E+02	−1.66E+02	−5.71E+01	−1.14E+02	−5.98E+01	−1.14E+02	−5.25E+01	−4.71E+01

Table A3
Stream tables of the SR section.

		1	2	3	4	5	6	7	8	9	10
T	K	295.2	295.2	294.5	295.2	409.4	295.9	321.3	321.7	533.0	298.5
p	bar	20.000	20.000	2.700	20.000	50.000	35.000	35.000	50.000	49.400	50.000
$\dot{m}$	kg/s	1.33	0.12	0.12	1.22	1.22	2.60	4.85	4.85	4.85	0.51
$\dot{n}$	kmol/s	0.20	0.02	0.02	0.19	0.19	0.14	0.27	0.27	0.27	0.03
vf		1.00	1.00	1.00	1.00	1.00	0.00	0.00	0.00	0.13	1.00
e_{ph}	kJ/kmol	7.42E+03	7.42E+03	2.43E+03	7.42E+03	1.03E+04	8.28E+01	1.53E+02	1.92E+02	6.55E+03	9.49E+03
e_{ch}	kJ/kmol	2.81E+05	2.81E+05	2.81E+05	2.81E+05	2.81E+05	1.21E+04	6.95E+03	6.95E+03	3.34E+01	8.32E+05
$\dot{E}$	kJ/s	5.85E+04	5.04E+03	4.95E+03	5.34E+04	5.40E+04	1.75E+03	1.90E+03	1.92E+03	3.90E+03	2.65E+04
h	kJ/kmol	−3.28E+04	−3.28E+04	−3.28E+04	−3.28E+04	−2.92E+04	−2.85E+05	−2.85E+05	−2.85E+05	−2.61E+05	−7.54E+04
s	kJ/kmol K	−2.74E+01	−2.74E+01	−1.06E+01	−2.74E+01	−2.48E+01	−1.72E+02	−1.64E+02	−1.64E+02	−1.10E+02	−1.15E+02

		11	12	13	14	15	16	17	18	19	20
T	K	456.4	773.3	1223.2	583.0	623.2	450.0	456.4	350.0	350.0	350.2
p	bar	49.300	49.000	48.500	48.200	47.700	47.100	49.300	46.000	46.000	35.000
$\dot{m}$	kg/s	6.58	6.58	6.58	6.58	6.57	6.57	6.58	3.29	3.28	2.26
$\dot{n}$	kmol/s	0.48	0.48	0.57	0.57	0.57	0.57	0.48	0.39	0.18	0.13
vf		0.59	1.00	1.00	1.00	1.00	0.86	0.46	1.00	0.00	0.00
e_{ph}	kJ/kmol	7.45E+03	1.63E+04	2.72E+04	1.22E+04	1.29E+04	9.31E+03	7.45E+03	9.63E+03	4.53E+02	4.29E+02

<div align="right">(continued on next page)</div>

Table A3 (*continued*)

		11	12	13	14	15	16	17	18	19	20
e_{ch}	kJ/kmol	1.65E+05	1.68E+05	1.51E+05	1.51E+05	1.50E+05	1.49E+05	1.65E+05	2.17E+05	1.01E+03	1.01E+03
$\dot{E}$	kJ/s	8.38E+04	8.94E+04	1.02E+05	9.35E+04	9.29E+04	9.04E+04	8.38E+04	8.84E+04	2.67E+02	1.81E+02
h	kJ/kmol	−1.60E+05	−1.34E+05	−8.16E+04	−1.04E+05	−1.05E+05	−1.16E+05	−1.60E+05	−5.50E+04	−2.84E+05	−2.84E+05
s	kJ/kmol K	−7.40E+01	−2.30E+01	1.22E+01	−1.40E+01	−1.40E+01	−3.63E+01	−7.40E+01	−2.18E+01	−1.57E+02	−1.57E+02

		21	22	23	24	25	26	27	28	29	30
T	K	350.2	350.0	350.0	350.0	350.0	305.0	295.0	408.5	389.2	1253.4
p	bar	35.000	44.500	44.500	44.500	2.700	2.300	1.013	2.400	2.400	2.100
$\dot{m}$	kg/s	1.02	0.58	0.49	0.08	2.71	0.03	9.82	9.85	12.67	12.67
$\dot{n}$	kmol/s	0.06	0.29	0.25	0.04	0.10	0.00	0.34	0.34	0.46	0.46
vf		0.00	1.00	1.00	1.00	1.00	1.00	1.00	1.00	1.00	1.00
e_{ph}	kJ/kmol	4.29E+02	9.57E+03	9.57E+03	9.57E+03	2.56E+03	2.02E+03	6.05E-01	2.62E+03	2.49E+03	2.02E+04
e_{ch}	kJ/kmol	1.01E+03	2.36E+05	2.36E+05	2.36E+05	1.67E+05	6.97E+05	1.07E+02	1.65E+03	4.75E+04	4.75E+04
$\dot{E}$	kJ/s	8.16E+01	7.05E+04	6.02E+04	1.03E+04	1.74E+04	5.44E+02	3.67E+01	1.46E+03	2.31E+04	3.13E+04
h	kJ/kmol	−2.84E+05	1.55E+03	1.55E+03	1.55E+03	−2.13E+05	−2.08E+05	−9.86E+01	2.76E+03	−4.65E+04	−1.65E+04
s	kJ/kmol K	−1.57E+02	−2.69E+01	−2.69E+01	−2.69E+01	7.72E+00	−6.14E+01	3.70E+00	6.07E+00	1.09E+01	5.18E+01

		31	32	33	34	35	36	37	38	39	40
T	K	1362.5	1300.0	425.0	298.5	298.5	314.7	552.0	585.0	580.1	646.2
p	bar	1.600	1.300	1.000	1.013	1.713	1.063	70.000	70.000	20.000	20.000
$\dot{m}$	kg/s	12.68	12.68	12.68	80.00	80.00	80.00	0.56	0.56	2.63	2.63
$\dot{n}$	kmol/s	0.44	0.44	0.44	4.44	4.44	4.44	0.03	0.03	0.15	0.15
vf		1.00	1.00	1.00	0.00	0.00	0.00	0.00	1.00	1.00	1.00
e_{ph}	kJ/kmol	2.36E+04	2.12E+04	6.40E+02	0.00E+00	1.68E+00	3.68E+01	6.98E+03	1.17E+04	9.89E+03	1.12E+04
e_{ch}	kJ/kmol	2.89E+03	2.89E+03	2.89E+03	9.00E+02	9.00E+02	9.00E+02	9.00E+02	9.50E+03	9.50E+03	9.50E+03
$\dot{E}$	kJ/s	1.15E+04	1.05E+04	1.54E+03	4.00E+03	4.00E+03	4.16E+03	2.45E+02	6.60E+02	2.83E+03	3.02E+03
h	kJ/kmol	−6.47E+04	−6.72E+04	−9.90E+04	−2.89E+05	−2.89E+05	−2.87E+05	−2.65E+05	−2.35E+05	−2.33E+05	−2.30E+05
s	kJ/kmol K	5.07E+01	5.05E+01	1.29E+01	−1.71E+02	−1.71E+02	−1.66E+02	−1.14E+02	−5.98E+01	−4.70E+01	−4.29E+01

Table A4
Exergy balances of the plant components.

Component	Product exergy streams	Fuel exergy streams
HT-PUMP1	$\dot{E}^{(2)} - \dot{E}^{(1)}$	Electricity
HT-COMPR	$\dot{E}^{(5)} - \dot{E}^{(4)}$	Electricity
HXC-HT1	$\dot{E}^{(7)} - (\dot{E}^{(3)} + \dot{E}^{(5)})$	$\dot{E}^{(12)} - \dot{E}^{(13)}$
HTREACT1	$\dot{E}^{(19)} - \dot{E}^{(18)} + \dot{E}_{ph}^{(8)} - \dot{E}_{ph}^{(7)}$	$\dot{E}_{ch}^{(7)} - \dot{E}_{ch}^{(8)}$
HT-VALVE	—	$\dot{E}^{(9)} - \dot{E}^{(10)}$
HXC-HT2	$\dot{E}^{(9)} - \dot{E}^{(8)}$	$\dot{E}^{(11)} - \dot{E}^{(12)}$
HTREACT2	$\dot{E}^{(20)} - \dot{E}^{(19)} + \dot{E}^{(25)} - \dot{E}^{(24)}$	$\dot{E}^{(10)} - \dot{E}^{(11)}$
HXC-HT3	$\dot{E}^{(3)} - \dot{E}^{(2)}$	$\dot{E}^{(13)} - \dot{E}^{(14)}$
HXC-HT4	$\dot{E}^{(23)} - \dot{E}^{(22)}$	$\dot{E}^{(14)} - \dot{E}^{(15)}$
HT-FLASH	—	$\dot{E}^{(15)} - (\dot{E}^{(16)} + \dot{E}^{(17)})$
HT-PUMP2	$\dot{E}^{(22)} - \dot{E}^{(21)}$	Electricity
HT section	$\dot{E}^{(16)} + \dot{E}^{(17)} + \dot{E}^{(20)} - \dot{E}^{(18)} + \dot{E}^{(25)} - \dot{E}^{(24)} + \dot{E}^{(23)} - \dot{E}^{(21)} - \dot{E}^{(1)}$	$\dot{E}^{(4)} +$ **electricity**
HC-COMPR	$\dot{E}^{(16)} - \dot{E}^{(15)}$	Electricity
HC-PUMP1	$\dot{E}^{(23)} - \dot{E}^{(22)}$	Electricity
HC-FLASH	—	$\dot{E}^{(1)} + \dot{E}^{(21)} - \dot{E}^{(2)} - \dot{E}^{(3)}$
HC-VALV1	—	$\dot{E}^{(3)} - \dot{E}^{(4)}$
HXC-HC1	$\dot{E}^{(5)} - \dot{E}^{(4)}$	$\dot{E}^{(20)} - \dot{E}^{(21)}$
HXC-HC2	$\dot{E}^{(6)} - \dot{E}^{(5)}$	$\dot{E}^{([SR]16)} - \dot{E}^{([SR]17)}$
HC-DIST1	$\dot{E}_{ch}^{(9)} + \dot{E}_{ch}^{(8)} + \dot{E}_{ch}^{(7)} - \dot{E}_{ch}^{(6)} + \dot{m}^{(7)} * (\overline{e}_{ph}^{(7)} - \overline{e}_{ph}^{(6)}) + \dot{m}^{(9)} * (\overline{e}_{ph}^{(9)} - \overline{e}_{ph}^{(6)}) + \dot{E}^{(24)} - \dot{E}^{(23)}$	$\dot{E}^{(26)} - \dot{E}^{(27)} + \dot{m}^{(8)} * (\overline{e}_{ph}^{(6)} - \overline{e}_{ph}^{(8)})$
HC-VALV2	—	$\dot{E}^{(9)} - \dot{E}^{(10)}$
HC-DIST2	$\dot{E}_{ch}^{(11)} + \dot{E}_{ch}^{(13)} - \dot{E}_{ch}^{(10)} + \dot{m}^{(13)} * (\overline{e}_{ph}^{(13)} - \overline{e}_{ph}^{(10)}) + \dot{E}^{(25)} - \dot{E}^{(24)}$	$\dot{E}^{(28)} - \dot{E}^{(29)} + \dot{m}^{(11)} * (\overline{e}_{ph}^{(10)} - \overline{e}_{ph}^{(11)})$
HC-PUMP2	$\dot{E}^{(12)} - \dot{E}^{(11)}$	Electricity
HC-PUMP3	$\dot{E}^{(14)} - \dot{E}^{(13)}$	Electricity
HC-REACT	$\dot{E}^{(31)} - \dot{E}^{(30)}$	$\dot{E}^{(17)} - \dot{E}^{(18)}$
HXC-HC3	$\dot{E}^{(17)} - (\dot{E}^{(14)} + \dot{E}^{(16)})$	$\dot{E}^{(19)} - \dot{E}^{(20)}$
HC-VALV3	—	$\dot{E}^{(18)} - \dot{E}^{(19)}$
HC section	$\dot{E}^{(2)} + \dot{E}^{(7)} + \dot{E}^{(8)} + \dot{E}^{(12)} + \dot{E}^{(31)} - \dot{E}^{(30)} + \dot{E}^{(25)} - \dot{E}^{(22)} - \dot{E}^{(1)}$	$\dot{E}^{(15)} + \dot{E}^{(26)} - \dot{E}^{(27)} + \dot{E}^{(28)} - \dot{E}^{(29)} +$ **electricity**
SR-MIX1	—	$\dot{E}^{(6)} + \dot{E}^{(20)} - \dot{E}^{(7)}$
SR-PUMP2	$\dot{E}^{(8)} - \dot{E}^{(7)}$	Electricity
SR-COMP1	$\dot{E}^{(5)} - \dot{E}^{(4)}$	Electricity
SR-MIX2	—	$\dot{E}^{(5)} + \dot{E}^{(9)} + \dot{E}^{(10)} - \dot{E}^{(11)}$
HXC SR-2	$\dot{E}^{(21)} - \dot{E}^{(11)}$	$\dot{E}^{(13)} - \dot{E}^{(14)}$
SR-VALV1	—	$\dot{E}^{(2)} - \dot{E}^{(3)}$

Table A4 (*continued*)

Component	Product exergy streams	Fuel exergy streams
SR-REACT	$\dot{E}^{(13)} - \dot{E}^{(12)}$	$\dot{E}^{(30)} - \dot{E}^{(31)}$
SR-WGS	$\dot{E}^{(40)} - \dot{E}^{(39)}$	$\dot{E}^{(14)} - \dot{E}^{(15)}$
HXC SR-1	$\dot{E}^{(9)} - \dot{E}^{(8)}$	$\dot{E}^{(15)} - \dot{E}^{(16)}$
SR-COMP2	$\dot{E}^{(28)} - (\dot{E}^{(26)} + \dot{E}^{(27)})$	Electricity
SR-COND	$\dot{E}^{(36)} - \dot{E}^{(35)}$	$\dot{E}^{(17)} - (\dot{E}^{(18)} + \dot{E}^{(19)})$
SR-PSA	–	$\dot{E}^{(22)} + \dot{E}^{(25)} - \dot{E}^{(18)}$
HXC SR-4	$\dot{E}^{(38)} - \dot{E}^{(37)}$	$\dot{E}^{(31)} - \dot{E}^{(32)}$
HXC SR-3	$\dot{E}^{(30)} - \dot{E}^{(29)}$	$\dot{E}^{(32)} - \dot{E}^{(33)}$
SR-MIX3	–	$\dot{E}^{(3)} + \dot{E}^{(25)} + \dot{E}^{(28)}$
SR-PUMP1	$\dot{E}^{(35)} - \dot{E}^{(34)}$	Electricity
SR-H2SPL	–	$\dot{E}^{(22)} - \dot{E}^{([HC]15)} - \dot{E}^{([HT]4)}$
SR section	$\dot{E}^{(23)} + \dot{E}^{(24)} + \dot{E}^{(38)} - \dot{E}^{(37)} + \dot{E}^{(40)} - \dot{E}^{(39)} + \dot{E}^{(36)} - \dot{E}^{(34)} + \dot{E}^{(33)} - \dot{E}^{(27)}$	$\dot{E}^{(1)} + \dot{E}^{(26)} + \dot{E}^{(10)} + \dot{E}^{(6)} + \textbf{electricity} + \dot{E}^{(6)} - \dot{E}^{(21)}$
Overall	$\dot{E}^{([HC]8)} + \dot{E}^{([HC]12)} + \dot{E}^{([SR]40)} + \dot{E}^{(PyrChar)} - \dot{E}^{([HT]18)}$	$\dot{E}^{(biomass)} + \dot{E}^{([SR]10)} + \textbf{electricity}$

References

[1] EC. Directive 2009-28-EC on the promotion of the use of energy from renewable sources. Brussels, Belgium: European Parliament and the Council; 2009.

[2] Bauen A, Berndes G, Junginger M, Londo M, Vuille F. Bioenergy – a sustainable and reliable energy source. IEA bioenergy report 2009:06. Rotorua, New Zealand. 2009.

[3] EEA. EU bioenergy potential from a resource efficiency perspective – EEA report no 6/2013. Copenhagen, Denmark. 2013.

[4] Eisentraut A. Sustainable production of second generation biofuels – potential and perspectives in major economies and developing countries. Paris, France: International Energy Agency; 2010.

[5] Venderbosch RH, Prins W. Fast pyrolysis technology development. Biofuel Bioprod Bior 2010;4:178–208.

[6] Jones SB, Valkenburg C, Walton CW, Elliott DC, Holladay JE, Stevens DJ, et al. Production of gasoline and diesel from biomass via fast pyrolysis, hydrotreating and hydrocracking: a design case. Washington, United States: Pacific Northwest National Laboratory; 2009.

[7] Wright MM, Daugaard DE, Satrio JA, Brown RC. Techno-economic analysis of biomass fast pyrolysis to transportation fuels. Fuel 2010;89:S2–10.

[8] Anex RP, Aden A, Kazi FK, Fortman J, Swanson RM, Wright MM, et al. Techno-economic comparison of biomass-to-transportation fuels via pyrolysis, gasification, and biochemical pathways. Fuel 2010;89:29–35.

[9] Peters JF, Iribarren D, Dufour J. Life cycle assessment of pyrolysis oil applications. Biomass Convers Bioref 2015. http://dx.doi.org/10.1007/s13399-014-0120-z. in press.

[10] Peters JF, Iribarren D, Dufour J. Simulation and life cycle assessment of biofuel production via fast pyrolysis and hydroupgrading. Fuel 2015;139:441–56.

[11] Bridgwater AV. Review of fast pyrolysis of biomass and product upgrading. Biomass Bioenerg 2012;38:68–94.

[12] Meier D, van de Beld B, Bridgwater AV, Elliott DC, Oasmaa A, Preto F. State-of-the-art of fast pyrolysis in IEA bioenergy member countries. Renew Sustain Energy Rev 2013;20:619–41.

[13] Iribarren D, Petrakopoulou F, Dufour J. Environmental and thermodynamic evaluation of CO2 capture, transport and storage with and without enhanced resource recovery. Energy 2013;50:477–85.

[14] Petrakopoulou F, Tsatsaronis G. Production of hydrogen-rich fuels for precombustion carbon capture in power plants: a thermodynamic assessment. Int J Hydrogen Energy 2012;37:7554–64.

[15] Velásquez-Arredondo HI, De Oliveira Junior S, Benjumea P. Exergy efficiency analysis of chemical and biochemical stages involved in liquid biofuels production processes. Energy 2012;41:138–45.

[16] Palacios-Bereche R, Mosqueira-Salazar KJ, Modesto M, Ensinas AV, Nebra SA, Serra LM, et al. Exergetic analysis of the integrated first- and second-generation ethanol production from sugarcane. Energy 2013;62:46–61.

[17] Tan HT, Lee KT, Mohamed AR. Second-generation bio-ethanol (SGB) from Malaysian palm empty fruit bunch: energy and exergy analyses. Bioresour Technol 2010;101:5719–27.

[18] Saidur R, BoroumandJazi G, Mekhilef S, Mohammed HA. A review on exergy analysis of biomass based fuels. Renew Sustain Energy Rev 2012;16:1217–22.

[19] Spyrakis S, Panopoulos KD, Kakaras E. Synthesis, modeling and exergy analysis of atmospheric air blown biomass gasification for Fischer–Tropsch process. Int J Thermodyn 2009;12:187–92.

[20] Ptasinski KJ. Thermodynamic efficiency of biomass gasification and biofuels conversion. Biofuel Bioprod Bioref 2008;2:239–53.

[21] Prins MJ, Ptasinski KJ, Janssen FJ. Exergetic optimisation of a production process of Fischer–Tropsch fuels from biomass. Fuel Process Technol 2005;86:375–89.

[22] Peters JF, Petrakopoulou F, Dufour J. Exergetic analysis of a fast pyrolysis process for bio-oil production. Fuel Process Technol 2014;119:245–55.

[23] Aspen Technology. Aspen Plus. 2012.

[24] Elliott DC. Historical developments in hydroprocessing bio-oils. Energy Fuel 2007;21:1792–815.

[25] Halder Topsoe. Hydrocracking catalysts 3. Lyngby, Denmark: Halder Topsoe A/S; 2013.

[26] Vaidyanathan S. Hydrocracking – an overview. In: 12th AICHE spring meeting. Houston, United States: Fluor; 2012.

[27] Molburg JC, Doctor RD. Hydrogen from steam-methane reforming with CO2 capture. In: 20th annual international Pittsburgh coal conference, Pittsburgh, United States; 2003.

[28] Sarkar S, Kumar A. Large-scale biohydrogen production from bio-oil. Bioresour Technol 2010;101:7350–61.

[29] Bejan A, Tsatsaronis G, Moran M. Thermal design and optimization. Wiley and Sons; 1996.

[30] Tsatsaronis G, Czielsa F. Thermoeconomics. Encyclopedia of physical science and technologyvol. 16; 2002. p. 659–80.

[31] Dincer I, Rosen MA. Thermodynamic fundamentals. In: Dincer I, Rosen MA, editors. Exergy–Energy, environment and sustainable development. Amsterdam, The Netherlands: Elsevier Ltd; 2013. p. 1–20.

[32] Govin OV, Diky VV, Kabo GJ, Blokhin AV. Evaluation of the chemical exergy of fuels and petroleum fractions. J Therm Anal Calorim 2000;62:123–33.

[33] Morris DR, Szargut J. Standard chemical exergy of some elements and compounds on the planet earth. Energy 1986;11:733–55.

[34] Kotas TJ. Exergy method of thermal plant analysis. Krieger Publishing Company; 1995.

[35] Ahrendts J. Reference states. Energy 1980;5:666–77.

[36] Dincer I, Rosen MA. Exergy (second edition) – energy, environment and sustainable development. 2nd ed. Amsterdam, The Netherlands: Elsevier B.V.; 2013.

[37] Tsatsaronis G. Exergy and thermodynamic analysis. In: Frangopoulos CA, editor. Exergy, Energy system analysis, and optimization. EOLSS Publishers Company Ltd; 2009.

[38] Frangopoulos CA. Exergy, energy system analysis, and optimization, vol. 1. EOLSS Publishers Company Ltd; 2009.

[39] Gaggioli EF, Obert RA. Thermodynamics. 2nd rev ed. McGraw-Hill; 1963.

[40] Tsatsaronis G. Strength and limitations of exergy analysis. In: Bejan A, Mamut E, editors. Thermodynamic optimization of complex energy systems. Dordrecht, Netherlands: Kluwer Academic Publishers; 1999. p. 93–100.

[41] Dahmen N, Henrich E, Dinjus E, Weirich F. The bioliq® bioslurry gasification process for the production of biosynfuels, organic chemicals, and energy. Energ Sustain Soc 2012;2:1–44.

[42] Dincer I, Rosen MA. Exergy analysis of crude oil distillation systems. In: Dincer I, Rosen MA, editors. Exergy – energy, environment and sustainable development. Amsterdam, The Netherlands: Elsevier B.V.; 2013. p. 335–45.

[43] Piekarczyk W, Czarnowska L, Ptasiński K, Stanek W. Thermodynamic evaluation of biomass-to-biofuels production systems. Energy 2013;62:95–104.

[44] Vitasari CR, Jurascik M, Ptasinski KJ. Exergy analysis of biomass-to-synthetic natural gas (SNG) process via indirect gasification of various biomass feedstock. Energy 2011;36:3825–37.

[45] Leible L, Kälber S, Kappler G, Lange S, Nieke E, Proplesch P, et al. Kraftstoff, Strom und Wärme aus Stroh und Waldrestholz. Karlsruhe, Germany: KIT Institut für Technikfolgenabschätzung und Systemanalyse; 2007.

[46] Wright MM, Brown RC, Boateng AA. Distributed processing of biomass to bio-oil for subsequent production of Fischer–Tropsch liquids. Biofuel Bioprod Bioref 2008;2:229–38.

[47] Sohel MI, Jack MW. Thermodynamic analysis and potential efficiency improvements of a biochemical process for lignocellulosic biofuel production. Linköping, Sweden: World Renewable Energy Congress; 2011.

[48] Van Rens GLMA, Huisman GH, De Lathouder H, Cornelissen RL. Performance and exergy analysis of biomass-to-fuel plants producing methanol, dimethylether or hydrogen. Biomass Bioenerg 2011;35:S145–54.

[49] Sohel MI, Jack MW. Thermodynamic analysis of lignocellulosic biofuel production via a biochemical process: guiding technology selection and research focus. Bioresour Technol 2011;102:2617–22.

[50] Velásquez HI, de Oliveira S, Benjumea P. Exergy analysis of biofuels production routes. In: 20th international congress of mechanical engineering — COBEM, Gramado, Brazil; 2009.

[51] Modarresi A, Kravanja P, Friedl A. Exergy analysis of the production of lignocellulosic ethanol. In: 14th international conference on process integration, modelling and optimisation for energy saving and pollution reduction, Florence, Italy; 2011.

[52] Ensinas AV, Codina V, Marechal F, Albarelli J, Silva MA, Ensinasa Adriano V, Codina Victor, Marechal François, Albarelli Juliana, Silva Maria Aparecida. Chem Eng Trans 2013;35:523—8.

[53] Modarresi A, Kravanja P, Friedl A. Pinch and exergy analysis of lignocellulosic ethanol, biomethane, heat and power production from straw. Appl Therm Eng 2012;43:20—8.

[54] Sues A, Juraščík M, Ptasinski K. Exergetic evaluation of 5 biowastes-to-biofuels routes via gasification. Energy 2010;35:996—1007.